

# Reactive Blending of Nylon 6 and Modified Poly(styrene-*co*-maleic anhydride); Influence of Poly(styrene-*co*-maleic anhydride) Modification by Fatty Amine onto Blend Properties

I. KELNAR,<sup>1</sup> M. STEPHAN,<sup>2</sup> L. JAKISCH,<sup>2</sup> I. FORTELNÝ<sup>1</sup>

<sup>1</sup> Institute of Macromolecular Chemistry, Academy of Sciences of the Czech Republic, 162 06 Prague 6, Czech Republic

<sup>2</sup> Institute of Polymer Research Dresden e.V., Hohe Strasse 6, D-01069 Dresden, Germany

Received 27 November 1996; accepted 6 March 1997

**ABSTRACT:** Blends of PA 6 with SMA or with 12.5–100% fatty amine (C 18) modified SMA at compositions 95/5–60/40 were studied. Particle size of SMA dispersed in PA 6 matrix was around 0.1  $\mu\text{m}$  due to *in situ* compatibilizer formation. The strength and stiffness of the blends were higher and toughness unchanged in comparison with PA 6 values. Microscopic observations confirm that improvement of mechanical properties of PA 6 by addition of brittle SMA is due to plastic deformation of SMA particles that consume significant amounts of deformational energy. This cold drawing is caused by compressive stress evolved by bulk deformation; this stress should exceed the critical brittle-to-ductile fracture mode transition. In the blends studied, cold drawing apparently occurred when the developed stress was lower than the critical one. It is concluded that a very fine phase structure with an apparently strong interface makes the plastic deformation of dispersed SMA easier. © 1997 John Wiley & Sons, Inc. *J Appl Polym Sci* **66**: 555–562, 1997

## INTRODUCTION

The toughness of polymers is usually improved by incorporation of rubbery components, mostly in the form of fine dispersed particles, which initiate crazing or shear yielding of matrix material.<sup>1</sup> By both mechanisms, a large amount of impact energy is dissipated and the toughness is raised significantly. Unfortunately, the presence of low-modulus inclusions lowers the stiffness and usually strength also.

Appropriate combination of ductile matrix with a dispersed high-modulus brittle polymer can give a system having enhanced mechanical properties including toughness. Such a blend with well-balanced mechanical properties was first studied by Kurauchi and Ohta<sup>2</sup> in the case of polycarbonate (PC)/poly(styrene-*co*-acrylonitrile) (SAN); the impact energy was absorbed by large plastic deformation of dispersed brittle particles. The proposed “cold drawing concept” is based on the pressure dependence of brittle-to-ductile transition of polymers.<sup>2,3</sup> Further, bulk deformation of a system having ductile matrix-brittle inclusions involves compressive stress on the dispersed stiffer particles provided adequate differences exist between the components in both modulus and Poisson's ratio.<sup>4</sup> If this pressure exceeds some critical value (brittle-to-ductile transition pressure), the

---

Correspondence to: I. Kelnar.

Contract grant sponsor: Institute of Polymer Research Dresden (Germany).

Contract grant sponsor: Grant Agency of the Czech Republic; contract grant number 106/95/1315.

*Journal of Applied Polymer Science*, Vol. 66, 555–562 (1997)

© 1997 John Wiley & Sons, Inc.

CCC 0021-8995/97/030555-08

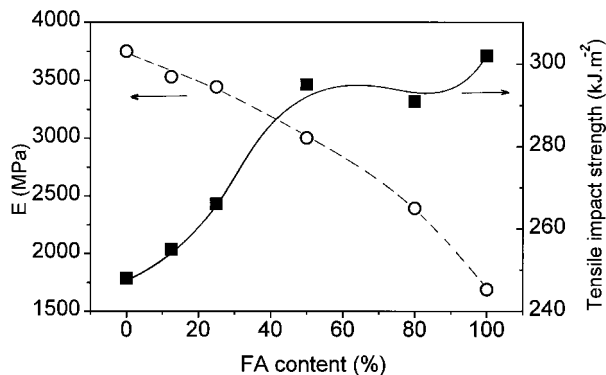


**Figure 1** Tensile modulus ( $E$ ) and tensile impact strength of SMA in dependence on the fatty amine content.

particles behave as if they were ductile. The particle size should not exceed  $\sim 2 \mu\text{m}$ ,<sup>5</sup> and good adhesion must exist between the phases, as was shown with the blend Nylon 6/SAN compatibilized with poly(styrene-*co*-maleic anhydride) (SMA) by Angola et al.<sup>6</sup>

Further studies<sup>5,7,8</sup> were oriented mainly to finding blends, where the “cold drawing concept” is active (i.e., enhanced strength and stiffness combined with higher than additive value of toughness), for example, blends of the PC matrix with SAN, poly(methyl methacrylate) (PMMA), acrylonitrile-butadiene-styrene copolymer (ABS) or polystyrene (PS) and blends of poly(butylene terephthalate) (PBT) with PMMA or SAN inclusions. Yamaoka<sup>9</sup> combined a ductile styrene-butadiene-styrene (SBS) matrix with brittle methyl methacrylate-styrene copolymer; here the deformational behavior was more complex due to the presence of elastomeric blocks in SBS.

Lu et al.<sup>10</sup> found an improvement of Nylon 6 properties by addition of SMA containing 8% maleic anhydride, Kim and Park<sup>11</sup> observed, with a similar blend (different Nylon 6 and blending conditions), an increase in the strength and decrease in toughness with increasing content of SMA. Chang and Hwu<sup>12</sup> found that, in the case of a Nylon 66/SMA blend, only modulus was increased over the Nylon 66 value.

This work is oriented predominantly to a more detailed study of the “cold drawing concept.” A blend of Nylon 6/SMA was chosen, due to the possibility of using a series of SMAs with increasing degree of modification of the anhydride group with fatty amine. Therefore, the influence of a gradual

change of dispersed brittle component properties on blend behavior could be studied.

## EXPERIMENTAL

### Materials

Polyamide 6 (PA6)—Ultramid B4 (BASF, Germany),  $M_n = 33,000$

Poly(styrene-*co*-maleic anhydride) (SMA)—Dylark 332 (Arco Chemical Co., USA), maleic anhydride content 14%,  $M_w = 90,000$ ,  $M_n = 180,000$

SMA modified with fatty (18 carbon atoms) amine (FA) containing 12.5; 25, and 50% FA (based on maleic anhydride content) was prepared according to Ref. 13 by reactive extrusion using twin-screw extruder ZSK 40 (Werner Pfleiderer, Germany). The temperature was in the range 230–240°C and residence time about 2 min.

Modifications with 80 and 100% FA were carried out in a *N,N*-dimethylacetamide solution heated to reflux for 6 h in the presence of triethylamine. The conversion rates were determined by FTIR-spectroscopy.

### Blend Preparation

Prior to mixing, PA 6 was dried for at least 12 h at 85°C in a vacuum oven. Mixing with SMA proceeded in the W 50 EH chamber of a Brabender Plasti-Corder at 250°C and 50 rpm for 10 min. After removing from the chamber and cooling in air, the obtained material was disintegrated in a mill and standard tensile bars (“dog bone” S2) were prepared by injection molding at 250°C using a two-compo-

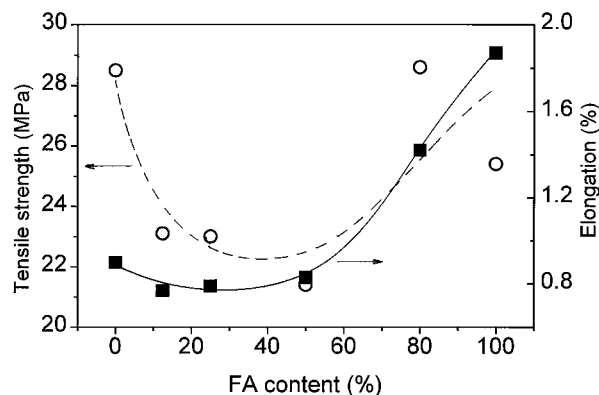


**Figure 2** Tensile strength and elongation at break of SMA in dependence on the fatty amine content.

**Table I Influence of Fatty Amine Modification on SMA Viscosity as Represented by the Torque in a Plastograph Brabender**

	Torque after 8 min (N.m)	Temperature (°C)
PA 6	13	250
SMA	11	235
SMA 12.5% FA	9	235
SMA 25% FA	6	235
SMA 50% FA	5	235
SMA 80% FA	3	230
SMA 100% FA	3	200

The main criterion for the selection of temperature was effective processing for subsequent preparation of samples for mechanical testing.

nent injection molding machine ES 200H80V/50HL2F (Engel Schwertberg, Austria).

**Mechanical Testing**

Tensile testing was carried out at 23°C using Zwick Z 010 apparatus and crosshead speed 15 mm/min. Poisson’s ratio of SMA was measured with two extensimeters and at a crosshead speed of 0.1 mm/min on strips 100 × 12 × 1 mm. Tensile impact strength ( $a_t$ ) was measured using unnotched samples (identical with those for tensile tests) and a pendulum PSD 50/15 (Heckert, Germany) according to DIN 53448. The maximum impact energy of the pendulum was 15J.

Morphological investigations were performed

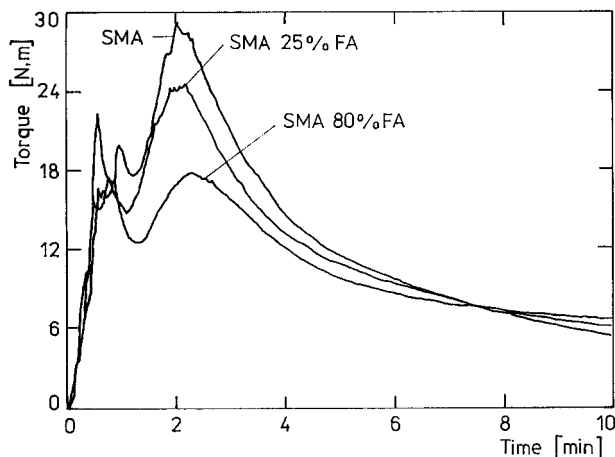


**Figure 3** Influence of SMA modification with fatty amine on the course of mixing of the PA6/SMA 70/30 blend in the Plastograph Brabender

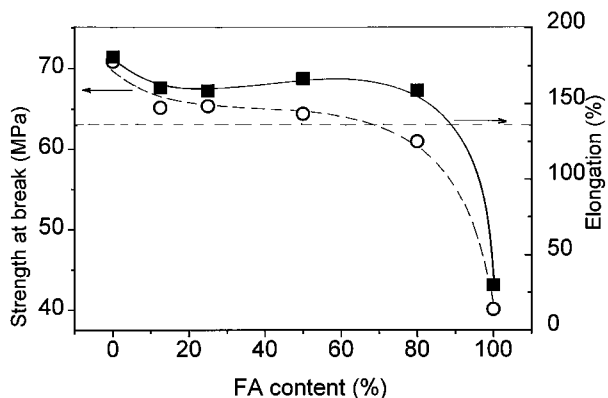


**Figure 4** Dependence of strength and elongation at break of PA6/SMA 70/30 blend on the fatty amine content. (Dashed line = strength at break of PA 6.)

with a scanning electron microscope JSM 35 on cryofractured samples. For better visualization of the SMA phase, etching in ethylmethyl ketone for 1 h was done.

**X-Ray Measurements**

The wide-angle X-ray (WAXS) measurements were performed using a HZG diffractometer (Freiberger Praezisionsmechanik, Freiberg, Germany). Small-angle X-ray (SAXS) experiments were carried out using a Kratky camera (A. Paar, Graz, Austria). In both cases Ni-filtered  $CuK_{\alpha}$  radiation and a proportional counter with energy discrimination was used.

**RESULTS AND DISCUSSION**

**Properties of Fatty Amine-Modified SMA**

From the lowering of stiffness and increase in tensile impact strength ( $a_t$ ) with growing FA content shown in Figure 1, it can be concluded that FA modification has a plasticizing effect on SMA. However, the material still remains brittle, as is demonstrated by the low level of elongation (Fig. 2), which is raised only with a higher degree of FA modification (over 50%). For strength, there is no clear tendency in this dependence (Fig. 2). Its initial lowering corresponds with plasticization, the subsequent increase at higher FA modification corresponds most probably with the above-mentioned higher elongability. FA modification also lowers the viscosity of SMA, as shown in Table I.

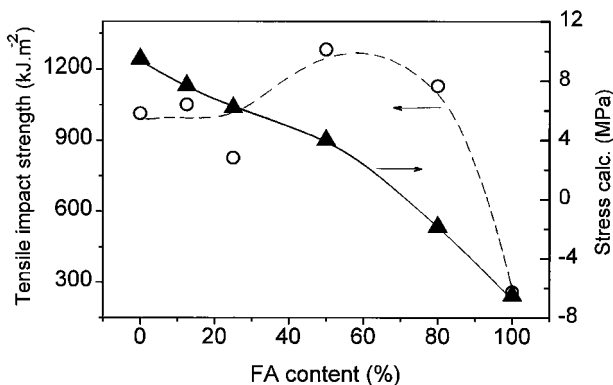


**Figure 5** Dependence of the tensile impact strength and calculated stress evolved on the SMA inclusion by bulk deformation of PA6/SMA 70/30 blend on the degree of SMA modification by fatty amine.

### Influence of SMA Modification on PA6/SMA Blend Properties

Influence of SMA modification on the blend properties was studied at a 70/30 composition.

The mixing curves (Fig. 3) reflect the existence of reaction between terminal amino groups of PA and MA (6). The first peak in the torque–time dependence represents plastification and heating, the second is the consequence of molecular weight increase (11) by *in situ* formation of PA 6–SMA copolymer. Lowering of the peak intensity with increasing FA content is due to the above-mentioned (Table I) lowering of SMA viscosity with simultaneous lower reactivity caused by modification. (Unfortunately, the imide concentration formed in the 70/30 blend was, without the copolymer extraction, below the sensitivity of the FTIR used.) From the dependencies in Figure 4 it is obvious that both strength ( $\sigma_B$ ) and elongation ( $\varepsilon_B$ ) are only slightly lowered by SMA modification up to the 80% FA content with a sharp decrease at 100% FA. Up to 50% FA in SMA, the blend strength is higher than that of PA 6.

Toughness (Fig. 5) shows a maximum at 50% FA, and again a decrease at 100% FA. The level of toughness of the blend is comparable with that of PA 6 (dotted line).

This observed decrease in  $\sigma_B$ ,  $\varepsilon_B$ , and  $a_t$  is in contrast with similar dependencies for unblended SMA on FA content (Figs. 1 and 2), where practically all three values attained their maximum with 100% FA modification. An explanation will be given in the subsequent section. As Figure 6 shows,  $E$  corresponds to plasticizing SMA by FA

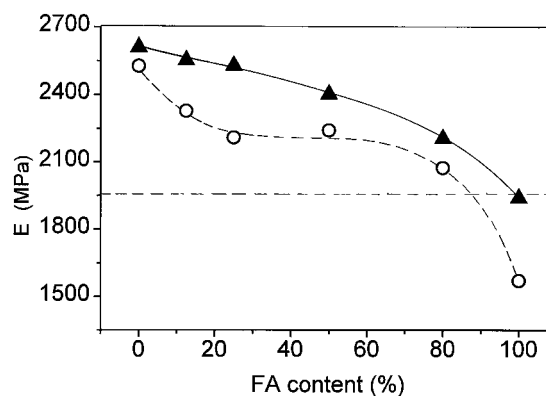
modification (Fig. 1) and practically follows Kerner's model<sup>14</sup> values (for modulus of a two-phase system with spherical inclusions) with only a slight deviation to lower value at 100% FA.

### Morphology of 70/30 Blend

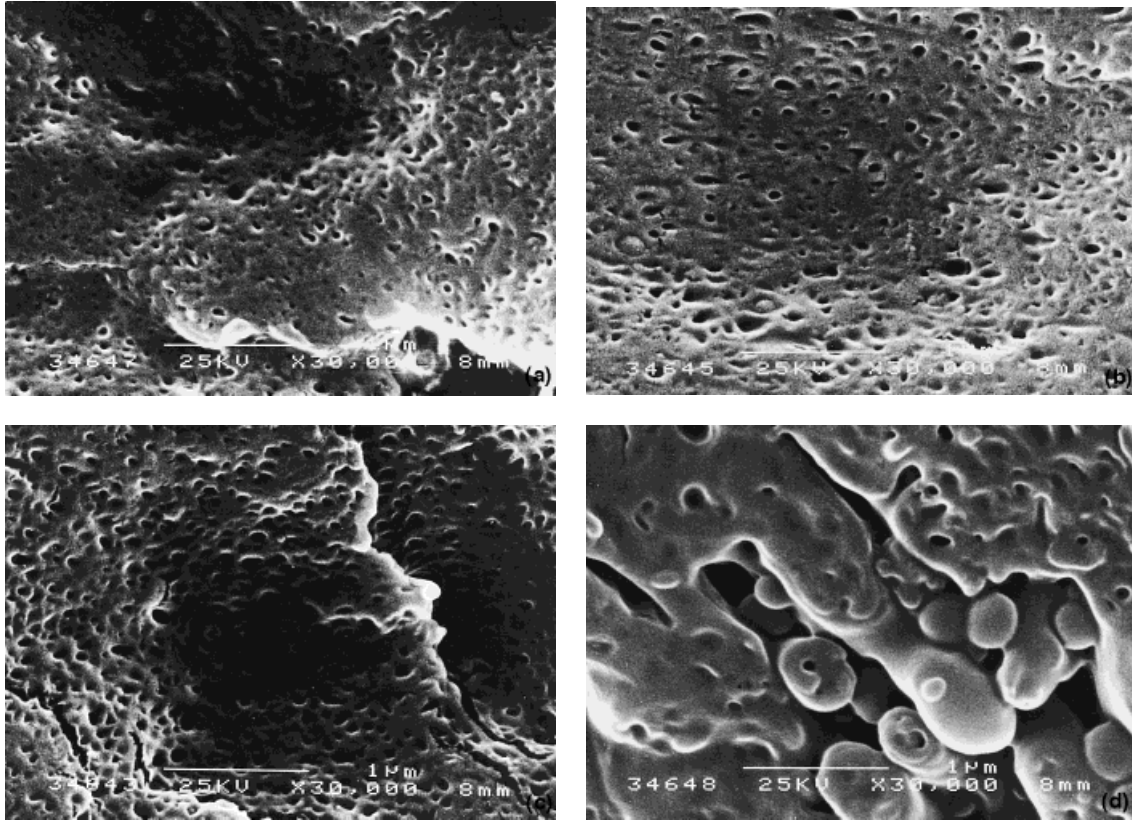
SEM observations (Fig. 7) show very small SMA inclusions (about 100 nm), which increase negligibly up to 80% FA modification. This situation is apparently a consequence of very effective compatibilization by *in situ* formed copolymer. However, the markedly rougher structure of the blend containing 100% FA-modified SMA [Fig. 7(d)] is undoubtedly responsible for the above-mentioned significant drop of its mechanical properties. One reason for this roughening is a too low viscosity of SMA with the highest FA modification (Table I); the ratio of blend component viscosities is apparently beyond the range necessary for effective mixing.<sup>15</sup> The second negative influence might be the zero content of unreacted MA in SMA, as indicated by FTIR, and, thus, no compatibilizer formation.

Figure 8 shows the morphology of the working part of a test specimen in the plane parallel to the force direction—the apparently elongated shape of SMA inclusions in the necked part clearly demonstrates the occurrence of the cold drawing mechanism. (The quality of pictures is adversely influenced by the fact that the observed dimensions are close to the resolution limits of the SEM used.)

In this respect, the influence of the change of SMA properties caused by FA modification on the



**Figure 6** Dependence of the tensile modulus of PA6/SMA 70/30 blend  $\circ$  and Kerner's model values  $\Delta$  on the degree of SMA modification by fatty amine. (Dashed line = value of PA 6.)



**Figure 7** Phase structure of 70/30 blends: (a) PA6/SMA, (b) PA6/SMA 50% FA, (c) PA6/SMA 80% FA, (d) PA6/SMA 100% FA.

stress on the dispersed particle by a uniaxial tensile deformation of the blend was evaluated.

According to Takahashi et al.,<sup>4</sup> the stress on the equatorial plane of a sphere through the differences in Young's modulus and Poisson's ratio between the dispersed sphere ( $E_2, \nu_2$ ) and the matrix ( $E_1, \nu_1$ ) is given as follows:

$$\sigma = [(3\lambda_2 + 2\mu_2)F + 2\mu_2GM]\varepsilon$$

where

$$M = -\frac{1}{3}(1 + \nu_1)$$

$$F = (1 - 2\nu_1)(\lambda_1 + 2\mu_1)/(4\mu_1 + 3\lambda_2 + 2\mu_2)$$

$$G = 15\mu_1(\lambda_1 + 2\mu_1)/[2\mu_2(3\lambda_1 + 8\mu_1) + \mu_1(9\lambda_1 + 14\mu_1)]$$

$$\mu_1 = \frac{E_1}{2(1 + \nu_1)}$$

$$\mu_2 = \frac{E_2}{2(1 + \nu_2)}$$

$$\lambda_1 = \nu_1 E_1 / (1 + \nu_1)(1 - 2\nu_1)$$

$$\lambda_2 = \nu_2 E_2 / (1 + \nu_2)(1 - 2\nu_2)$$

where  $\varepsilon$  is the experimental value of yield elongation (here a value of 4% was used).

From Figure 6 it is obvious that no break exists in the  $\sigma$  vs. SMA modification degree dependence. On the other hand, already between 50 and 80% FA modification of blended SMA, a change from compressive stress (here having positive values) to tensile stress occurs. Further, even the  $\sigma$  value of unmodified SMA ( $\sim 10$  MPa) is relatively low. Though the critical brittle-to-ductile transition stress ( $\sigma_c$ ) of SMA is not known, the value of its closest analog, PS, is about 50 MPa; therefore the  $\sigma_{\text{calc}}$  values found are apparently lower than  $\sigma_c$ . In spite of these findings, cold drawing of dispersed particles obviously exists (Fig. 8) in the blends studied.

This situation is in contrast with previous work<sup>5-8</sup> where, in blends of compatible components like PC/SAN having particle size 1–2  $\mu\text{m}$ , the  $\sigma_{\text{calc}}$  really had to exceed  $\sigma_c$  for cold drawing

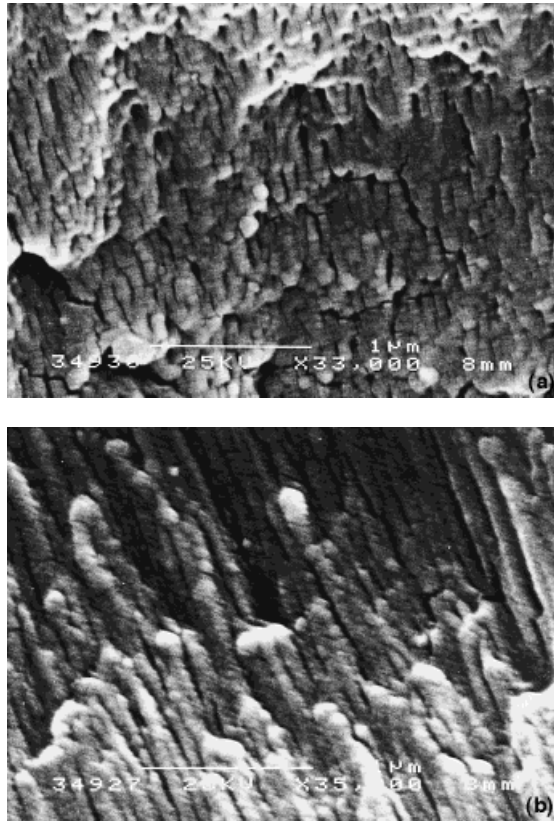


**Figure 8** Morphology of the elongated neck (parallel to straining force direction): (a) PA6/SMA 70/30 blend, (b) PA6/SMA-50% FA 70/30 blend.

to occur. Taking into account the observed phase structure (Figs. 7 and 8), it can be concluded that, in the case of such a well-compatibilized blend having far smaller particle size, the deformation of dispersed particles is easier, most probably due to a better stress transfer between the components, and to a possible “positive size effect” of submicron particles found.

#### Morphology Dependence on Blend Composition

Composition dependencies were studied with PA 6/SMA and SMA 50% FA blends in the range where PA 6 was expected to be a continuous matrix. SMA 50% FA was chosen due to its highest toughness value in the 70/30 blend (Fig. 6).

From Figure 9 it is obvious that the very fine size of dispersed SMA in the 90/10 blend (close to the limit of SEM resolution) is only slightly increased at a higher SMA content. The phase structure of both modified and unmodified SMA blends was practically the same with the excep-

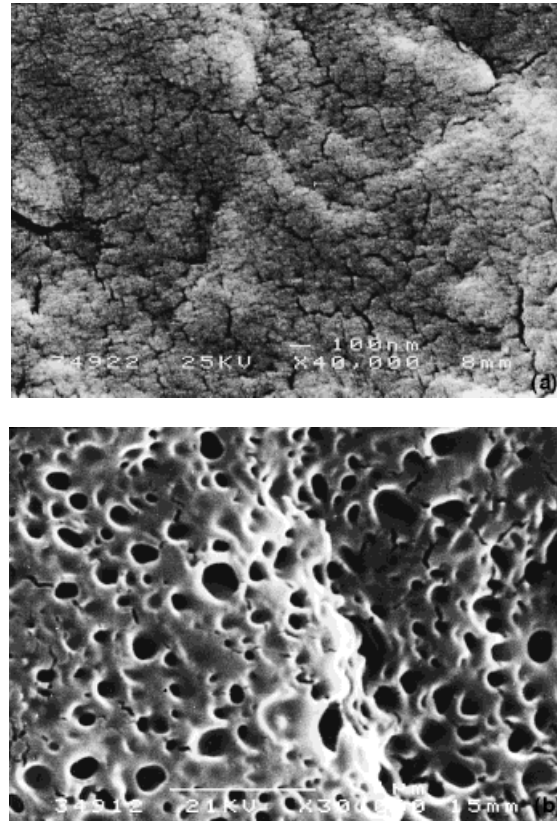


**Figure 9** Phase structure of PA6/SMA blend in dependence on the composition (a) 90/10, (b) 60/40, [70/30 blend is shown in Fig. 7(a)].

tion of the 60/40 PA6/SMA 50% FA blend, where the material was destroyed (disintegrated) during preparation, i.e., immersion in MEK for 1 h. This fact most probably indicates at least a co-continuous structure of this blend (with possible

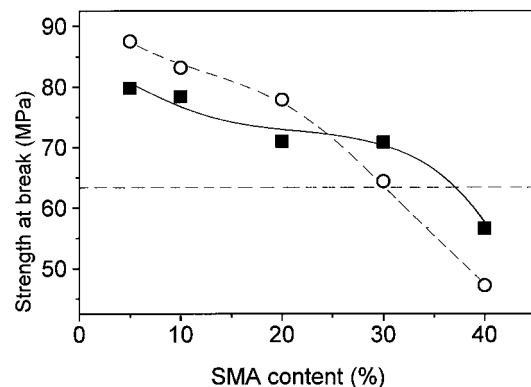


**Figure 10** Strength at break of PA6/SMA ■ and PA6/SMA-50% FA ○ blends in dependence on composition. (Dashed line = value of PA 6.)

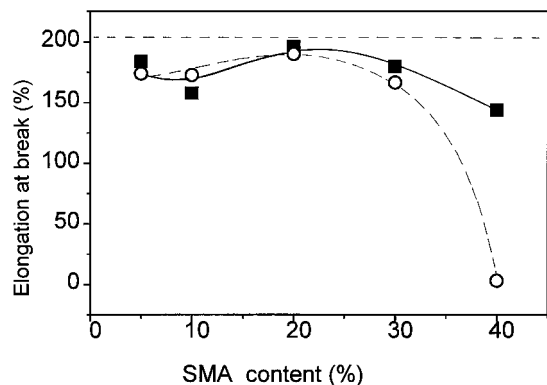


**Figure 11** Elongation at break of PA6/SMA ■ and PA6/SMA-50% FA ○ blends in dependence on composition. (Dashed line = value of PA 6.)

worsening of PA 6 crystallinity by high content of modified SMA).

In the case of strength (Fig. 10), of interest is the crossing of dependencies for both modified and unmodified SMA. Up to 75/25 composition, the PA6/SMA-50% FA blend has higher values, which are then exceeded by the PA6/SMA blend at the higher SMA concentrations, i.e., a higher content of fatty amine modified SMA worsens the blend strength. Elongation is practically the same for both unmodified and modified SMA blends up to 70/30 composition, as shown in Figure 11. The significantly lower  $\epsilon_B$  values for FA-modified SMA at 60/40 composition, with simultaneously observed brittle fracture (from stress-strain curves), obviously corresponds with the above-mentioned differences in the phase structure between the PA6/SMA and PA6/SMA-50% FA 60/40 blends.

Composition dependence of toughness (Fig. 12)

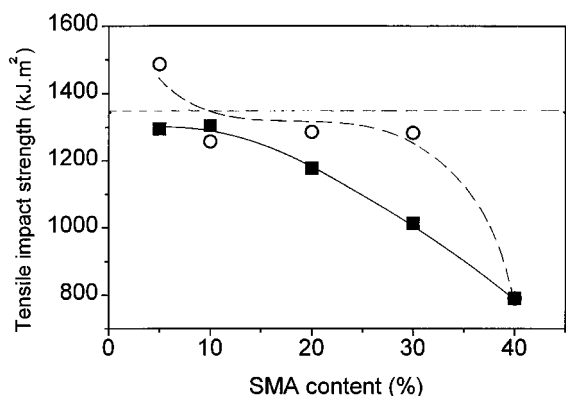


**Figure 12** Tensile impact strength of PA6/SMA ■ and PA6/SMA-50% FA ○ blends in dependence on composition. (Dashed line = value of PA 6).

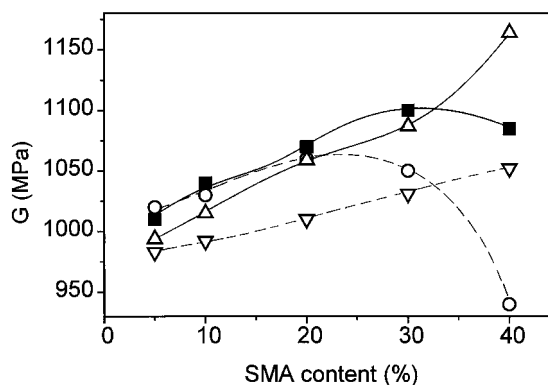


**Figure 13** Dependence of shear modulus on blend composition: PA6/SMA ■ and corresponding Kerner's model values  $\Delta$ , PA6/SMA-50% FA ○, and corresponding Kerner's model values  $\nabla$ .

reflects the more effective toughening of 50% FA-modified SMA; the value of its 95/5 blend exceeds that of PA 6. Significant lowering of  $a_t$  for 60/40 PA6/SMA-50% FA blend corresponds to the observed brittle fracture during tensile testing and to the changed phase structure mentioned above, too.

Figure 13 presents the concentration dependence of shear modulus ( $G$ ) of samples prepared from 1-mm thick plates pressed from material blended in a Brabender Plasti-Corder. Both dependencies contain a maximum, which is shifted to lower SMA contents in the case of 50% FA modification. The PA 6/SMA blends, up to the 30% SMA content, follow the dependence predicted by Kerner's model while modulus of the 60/40 blend is significantly lower.

For the modified SMA-containing blend, a slight lowering of  $G$  occurs already at the 70/30 composition, then a very sharp decrease is observed. Although the modified SMA blends, up to 80/20 composition, also followed the tendency

**Table II X-Ray Measurements**

PA/SMA-50% FA Blend Composition	Index Crystallinity	Supermolecular Periodicity (nm)
90/10	0.17	5.84
70/30	0.19	5.84
60/40	0.08	5.5
PA 6	0.25	5.84

Values are based on the PA 6 content.

given by Kerner's model, the difference between absolute modulus values (experimental and calculated) was greater than for unmodified blends (Fig. 12).

Due to the fact that morphology of both SMA and SMA-50% FA blends are practically the same up to 70/30 composition (including the PA6/SMA 60/40 blend), the explanation of these modulus dependencies could be a possible influencing of PA 6 crystallinity by the presence of SMA. As shown by X-ray diffraction results in Table II, the crystallinity of PA 6 in the blend is lower than that of the single polymer, with the lowest value found in the case of 60/40 composition. Similarly, the supermolecular periodicity (average thickness of the lamella with amorphous interlayer) attains its lowest value and small-angle reflection is broader with the 60/40 blend, i.e., the supermolecular structure of this sample is more disturbed also.

## CONCLUSIONS

Mechanical performance and morphological observations demonstrate that cold drawing of SMA and fatty amine-modified SMA particles, dispersed in PA 6 matrix, occurs even in the case of relatively close values of both component's moduli. Additionally, the stress evolved on the SMA particles by bulk deformation was lower than the critical brittle-to-ductile transition pressure. This finding is in contrast with previous studies where, in the blend with dispersed particle size 1–2  $\mu\text{m}$ , the stress had to exceed the critical value for the cold drawing (plastic deformation) to occur. The easier plastic deformation of SMA and modified SMA inclusions is explained by their very fine

dimensions, lower than 100 nm, and strong interface, both assuring perfect stress transfer between the components.

I.K. is grateful to the Institute of Polymer Research Dresden (Germany) for arranging his stay and financial support. I.F. thanks the Grant Agency of the Czech Republic (Grant No. 106/95/1315) for support.

## REFERENCES

1. C. B. Bucknall, *Toughened Plastics*, Applied Science Publishers, London, 1977.
2. T. Kurauchi and T. Ohta, *J. Mater. Sci.*, **19**, 1699 (1984).
3. K. Matsushige, S. V. Radcliffe, and E. Baer, *J. Appl. Polym. Sci.*, **20**, 1853 (1976).
4. K. Takahashi, M. Ikeda, K. Harakawa, and K. Tanaka, *J. Polym. Sci.*, **16**, 415 (1978).
5. K.-K. Koo, T. Inoue, and K. Miyasaka, *Polym. Eng. Sci.*, **25**, 741 (1985).
6. J. C. Angola, Y. Fujita, T. Sakai, and T. Inoue, *J. Polym. Sci. (B)*, **26**, 807 (1988).
7. Y. Fujita, K.-K. Koo, J. C. Angola, T. Inoue, and T. Sakai, *Kobunshi Ronbunshu*, **43**, 119 (1986).
8. C. Quingying, Z. Wenjun, and H.-G. Fritz, PPS Sixth Annual Meeting, Nice, France, Abstract P07–11.
9. I. Yamaoka, *Polymer*, **36**, 3359 (1995).
10. M. Lu, H. Keskkula, and D. R. Paul, *Polymer*, **34**, 1874 (1993).
11. B. K. Kim and S. J. Park, *J. Appl. Polym. Sci.*, **43**, 357 (1991).
12. F.-CH. Chang and Y.-CH. Hwu, *Polym. Eng. Sci.*, **31**, 1509 (1991).
12. L. Jakisch, D. Fischer, M. Stephan, and K.-D. Eichhorn, *Kunststoffe*, **85**, 1338 (1995).
13. E. H. Kerner, *Proc. Phys. Soc.*, **69**, 808 (1956).
14. J. Lyngaae-Jorgensen, in *Polymer Blends and Alloys*, M. J. Folkes and P. S. Hope, Eds., Blackie Academic and Professional, London 1993.